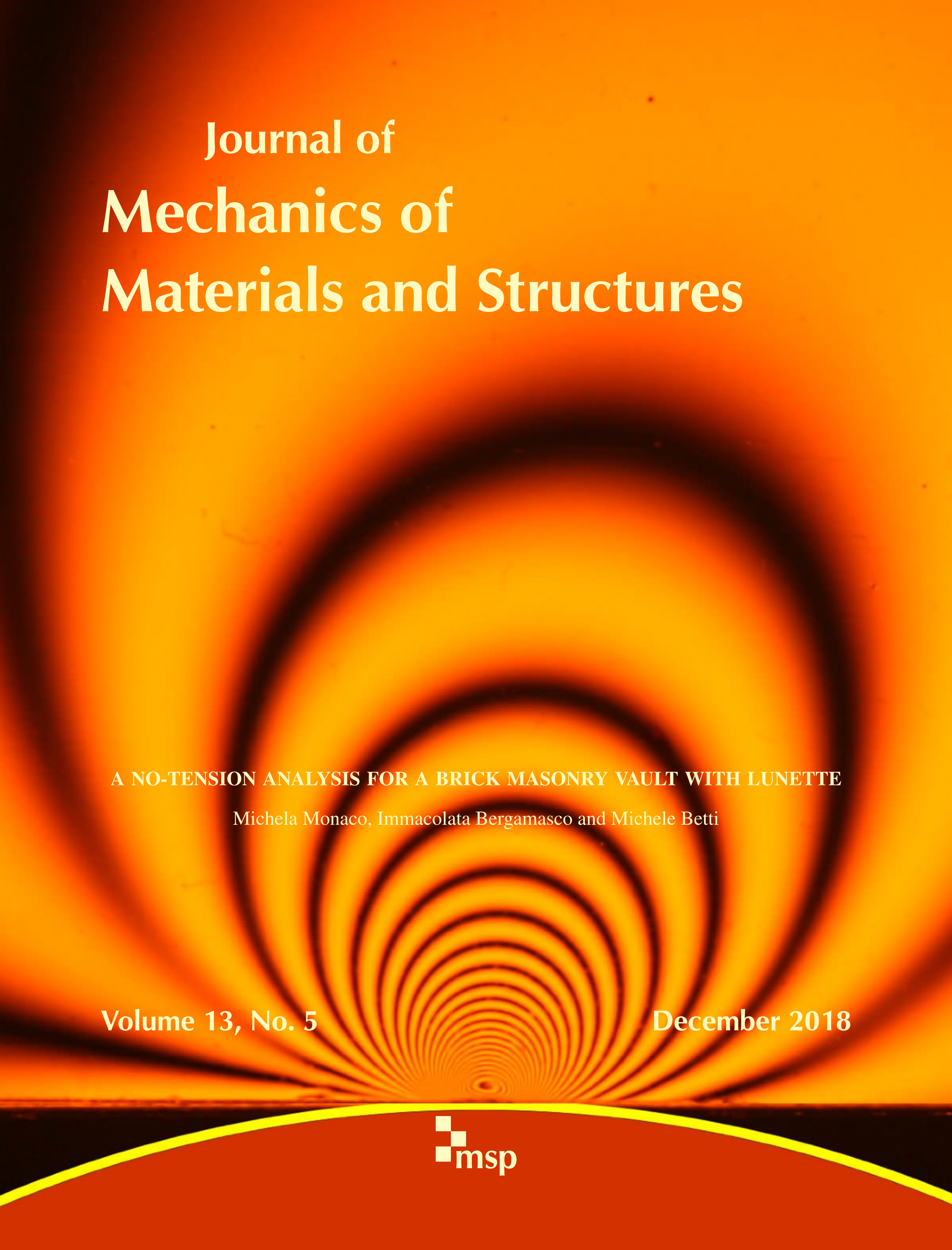

Journal of
Mechanics of Materials and Structures

A NO-TENSION ANALYSIS FOR A BRICK MASONRY VAULT WITH LUNETTE

Michela Monaco, Immacolata Bergamasco and Michele Betti

Volume 13, No. 5 December 2018

msp

JOURNAL OF MECHANICS OF MATERIALS AND STRUCTURES
Vol. 13, No. 5, 2018
dx.doi.org/10.2140/jomms.2018.13.703

A NO-TENSION ANALYSIS FOR A BRICK MASONRY VAULT WITH LUNETTE

MICHELA MONACO, IMMACOLATA BERGAMASCO AND MICHELE BETTI

A large class of analysis methods has been developed during the last century for the study of masonry structures. Among them, the so-called unilateral no-tension model plays a fundamental role. Starting from the pioneer papers by Heyman in the second half of sixties, a new definition of the safety factor based on the equilibrium of the masonry structure as a no-tension body has been considered. The safety of the structure is mainly determined by its geometry rather than its material strength. The funicular analysis largely used in the 19th century has been improved in light of Heyman's approach to obtain computational methods based on lower-bound solutions. Heyman's hypotheses are the basis of the rigid no-tension continuous approach presented and applied to a barrel vault with lunette in the San Barbaziano church in Bologna. The masonry vault is modelled as a membrane (thrust surface) subjected to compressive stresses only, contained within extrados and intrados surfaces, and carrying uniform applied loads. The geometry of the unilateral membrane, described as an unknown smooth surface, and the associated admissible stress field are determined via a concave stress function necessary for equilibrium and unilateral constraints fulfillment. Special attention has been devoted to the singular stress field arising in the curves at the intersection of the vaults.

1. Introduction

Appropriate and effective analysis methods for the assessment of masonry buildings are a necessary step in the preservation of what is generally defined as "cultural heritage" [Bergamasco et al. 2018]. A suitable calibration of interventions is in fact possible with reliable tools [Sacco et al. 2018]. They should take into account the specificity of the examined buildings, which, in general, presents peculiar aspects due to the presence of various particular geometries like vaults, arches, and isolated columns. Observation of several collapsed stone-block masonry structures, such as the temples at Selinunte and Agrigento, has shown that the major cause of global failure is loss of equilibrium rather than material failure [Como 1992], since in many cases the collapsed blocks are in perfect condition and restoration can be done by rebuilding [Heyman 1970]. This observation applies to masonry arches, vaults, and any other masonry structure that they may be a part of [Moseley 1833; 1860].

The use of arches can be traced back to 3000 BC and the earliest civilizations, in the marshlands of lower Egypt and Mesopotamia. Roman engineers used arches in aqueducts, theaters, amphitheaters, and temples, but perhaps the best structural use of arches is in bridges: the Pons Fabricius and Pons Cestius in Rome (Italy), the Alcantara and Abelterio bridges in Portugal, and the Pons Flavius in Saint Chamas (France) are only a few examples of the Roman solution to the problem of bridging a gap [Hendry 1995]. The same considerations can be applied to the masterpieces of Roman engineering: the masonry vaults. Several of these masonry structures remain in service, despite having been subjected for centuries to a

Keywords: combined masonry vaults, unilateral materials, membrane behaviour, singular stress fields.

heavy regime of environmental conditions and loadings [Gesualdo and Monaco 2010; Buonocore et al. 2014].

Very few masonry arches and vaults have been built in modern times, and knowledge of the related design methods is no longer part of a civil engineer's training [Huerta 2001]. Despite a growing need for rehabilitation and conservation of these structures, understanding of their behaviour has declined during the last century, and the available professional tools for assessing them are in some cases of questionable reliability [Gesualdo et al. 2010; Bartoli et al. 2017].

The equilibrium approach dates back to a small note of Robert Hooke [1676] under the mask of a cipher:

> "*The true Mathematical and Mechanichal form of all manner of Arches for Building, with the true butment necessary to each of them. A Problem which no Architectonick Writer hath ever yet attempted, much less performed*".

The cipher deciphered gives "*Ut pendet continuum flexile sic stabit contiguum rigidum inversum*". Ever since Hooke's statement, the equilibrium approach has been used to state that if a catenary shape can be included in the thickness of the arch, then the arch is in equilibrium.

Analytical and graphical methods have been applied since then for the analysis of masonry arch structures, although the methods of graphical statics have been the strongest tools used to solve the equilibrium problems of arches and vaults for centuries (for a thorough discussion on this aspect, see [Huerta 2008]). The seminal papers by Heyman [1966; 1977; 1982] gave a new definition of the equilibrium approach, including the analysis of vaulted structures in the general framework of limit analysis, and in particular in that of the safe theorem [Kurrer 2008]. The observation of the very low stress level in the masonry has induced Heyman's three basic hypotheses: infinite compressive strength, null tensile strength, and no sliding among voussoirs. If the masonry arch fulfills these requirements, and the structure is stable, there exists at least one thrust line contained in its cross section. The safety factor can be recognized as the ratio between the actual thickness of the structure and the minimum thickness necessary to contain a line of thrust.

Heyman's hypotheses are the basis of several classes of methods based on the safe theorem [Lucchesi et al. 2012]. Among them, the thrust network analysis (TNA), a methodology initiated by O'Dwyer [1999] and developed mainly by Block [Block 2009; Block and Lachauer 2014], should be mentioned, and it recently has been extended and applied to particular vaulted structures [Fraternali 2010; Marmo and Rosati 2017]. The equilibrium of vaulted structures is examined with reference to a network of thrusts in equilibrium with the applied loads. The same discrete approach has been developed in [Fraternali 2010; 2011], in which a sort of truss structure represents the continuous masonry vault. The stress field is approximated through a network of lumped stresses defined on the truss structure and the corresponding energy is defined at the truss nodes [Fraternali et al. 2014].

The second class of methods makes reference to the definition of a funicular membrane included in the masonry vault. It starts with the Pucher papers [1934; 1937], developed for reinforced concrete shells, and successively extended to masonry structures considered as rigid no-tension materials by Angelillo et al. [2013]. The modelling of masonry as a unilateral material dates back to Heyman's papers, but only recently, thanks to the development of computing efficiency, has it been successfully applied to complex masonry structures [Lucchesi et al. 2007; 2008; Angelillo et al. 2010]. A further list of references is given in [Angelillo et al. 2016; Iannuzzo et al. 2018]. Successive applications have been proposed to model helical stairs [Angelillo 2015; Gesualdo et al. 2017; Marmo et al. 2018] and combined masonry vaults [Bergamasco et al. 2017].

This paper presents a continuum equilibrium approach for a system of combined vaults. The aim is to determine a compressive thrust surface contained between extrados and intrados of the vault. The constitutive behaviour of the material is assumed as rigid no-tension. A statically admissible stress field (in equilibrium with the applied selfweight, i.e., the only load applied on the vault system) is determined. As a case study the barrel vault with lunette in the San Barbaziano church in Bologna is considered. Particular attention is given to the singular stress field in the form of line Dirac deltas along the intersection curves.

2. Statement of the problem

A masonry vault is a complex structure that can be analytically represented by a spatial domain whose boundaries are the intrados's and extrados's surfaces. The model here schematically illustrated (more details can be found in [Angelillo et al. 2013]) considers the vault as a membrane structure S contained in the domain whose thickness t coincides with the vault's. The problem takes into account two unknowns: the membrane shape S and the stress function F; the latter is determined by solving an Airy stress problem, as shown in the following. The geometry of the membrane S is given in the Monge form $x_3 = f(x_1, x_2)$. The function $f(x_1, x_2)$ is continuous on the two-dimensional connected definition domain Ω. The material point $\boldsymbol{x}$ on the membrane S has coordinates defined in the Cartesian reference system coherent with base $\boldsymbol{B} = \{\boldsymbol{e}_1, \boldsymbol{e}_2, \boldsymbol{e}_3\}$ as

$$\boldsymbol{x} = \{x_1, x_2, f(x_1, x_2)\}, \qquad \{x_1, x_2\} \in \Omega,$$

where Ω is the definition domain whose boundary $\partial\Omega$ is composed of a finite number of closed curves, with unit outer normal $\boldsymbol{n}$; $\{x_1, x_2\}$ are the coordinate components on the projection plane Ω of S; and $f(x_1, x_2) = x_3$ is the rise of the membrane with $f \in C^{\circ}(\Omega)$.

Figure 1 shows the surface with a detailed description of a differential element of the membrane. The loading system is represented by the external forces pressure $\boldsymbol{q} = \{q_1, q_2, q_3\}$.

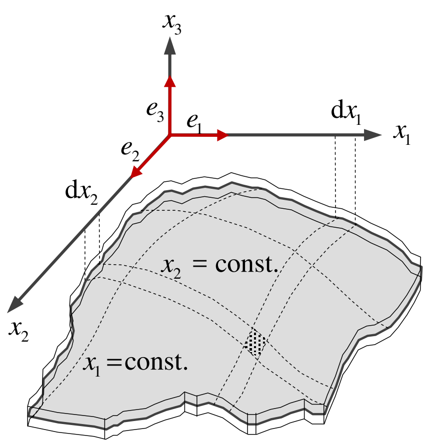

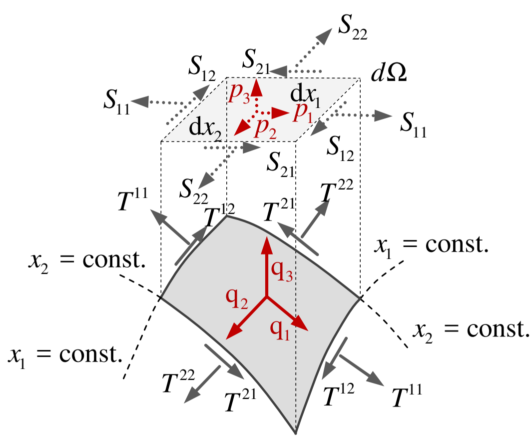

Figure 1. Left: membrane structure. Right: membrane stresses $T^{\alpha\beta}$ and Pucher stresses S_{ij}.

The membrane stress tensor $\boldsymbol{T} = \{T^{11}, T^{22}, T^{12}\}$ is defined in the covariant vector basis $\boldsymbol{A}$ tangent to S. Both the covariant $\boldsymbol{A}$ and the contravariant $\boldsymbol{A}^1$ vector bases [Pucher 1934] are reported below:

$$\boldsymbol{A} = \{\boldsymbol{a}_1, \boldsymbol{a}_2, \boldsymbol{a}_3\} = \begin{bmatrix} 1 & 0 & -f_{,1} \\ 0 & 1 & -f_{,2} \\ f_{,1}/J & f_{,2}/J & -1/J \end{bmatrix}, \quad \boldsymbol{A}^1 = \{\boldsymbol{a}^1, \boldsymbol{a}^2, \boldsymbol{a}_3\} = \frac{1}{J^2}\begin{bmatrix} 1+f_{,2}^2 & -f_{,1}f_{,2} & -f_{,1} \\ -f_{,1}f_{,2} & 1+f_{,1}^2 & -f_{,2} \\ Jf_{,1} & Jf_{,2} & -J \end{bmatrix}. \quad (1)$$

Here the comma in the subscripts indicates partial differentiation with respect to the variable x_i and $J = \sqrt{1 + f_{,1}^2 + f_{,2}^2}$ is the Jacobian determinant, i.e., the ratio between the differential surface area on S and its projection on the plane $f(x_1, x_2) = 0$.

A surface stress tensor $\boldsymbol{T}$ is determined for the generalised membrane stress on S and it is defined per unit length of horizontal line element in the covariant base $\boldsymbol{A}$ as

$$\boldsymbol{T} = T^{\alpha\beta}\boldsymbol{a}_\alpha \otimes \boldsymbol{a}_\beta,$$

where $T^{\alpha\beta}$ are the contravariant components of $\boldsymbol{T}$ with Einstein summation convention. The problem of equilibrium per unit area gives

$$\frac{\partial}{\partial x_\gamma}(T^{\alpha\beta}\boldsymbol{a}_\alpha \otimes \boldsymbol{a}_\beta)\,\boldsymbol{a}^\gamma + \boldsymbol{q} = \boldsymbol{0}. \quad (2)$$

Introducing the projected stress components $S_{\alpha\beta} = JT^{\alpha\beta}$ (Pucher stresses), after some manipulation, the system of equations (2) in the reference system $\{\boldsymbol{e}_1, \boldsymbol{e}_2, \boldsymbol{m} = \boldsymbol{a}_3\}$ becomes [Pucher 1934; 1937]

$$S_{11,1} + S_{12,2} + p_1 = 0, \qquad S_{21,1} + S_{22,2} + p_2 = 0, \qquad S_{\alpha\beta}\, f_{,\alpha\beta} - p_\gamma\, f_{,\gamma} + p_3 = 0, \quad (3)$$

where $\boldsymbol{p} = J\boldsymbol{q}$ is the pressure on the projected area. The plane stress problem can be recognized in the first two equations of the system (3), so that the solution can be obtained in terms of a single unknown function, i.e., an Airy stress function $F(x_1, x_2)$ so that

$$S_{11} = F_{,22}, \qquad S_{22} = F_{,11}, \qquad S_{12} = S_{21} = -F_{,12}. \quad (4)$$

The transverse equilibrium in terms of $F(x_1, x_2)$ is expressed by

$$L(F) = F_{,22}\, f_{,11} + F_{,11}\, f_{,22} - 2F_{,12}\, f_{,12} = p, \quad (5)$$

where the vertical force defined per unit horizontal area $\boldsymbol{p} = \{0, 0, -p\}$ and $L(F)$ has been called the Pucher operator [Flügge and Geyling 1957]. Stress restrictions due to the assumption of masonry material as a rigid no-tension one in the Heyman sense [1966] are assumed. In other words, the generalised stress $\boldsymbol{T}$ is negative semidefinite and does null work for the corresponding positive semidefinite strain $\boldsymbol{E}$:

$$\boldsymbol{T} \in \mathrm{Sym}^-, \quad \boldsymbol{E} \in \mathrm{Sym}^+, \quad \boldsymbol{T} \cdot \boldsymbol{E} = 0. \quad (6)$$

In terms of the stress function F, the unilateral constraints reduce to the relations

$$F_{,11} + F_{,22} \le 0, \quad F_{,11}\, F_{,22} - F_{,12}^2 \ge 0. \quad (7)$$

These correspond to the condition on $F(x_1, x_2)$ to be concave. The only requirement of continuity for F gives as a result the possibility of a folded surface, with discontinuous Pucher stresses defined as a Dirac delta line whose definition domain is the projection Γ of the fold. The Hessian $\boldsymbol{H}$ of F has a uniaxial

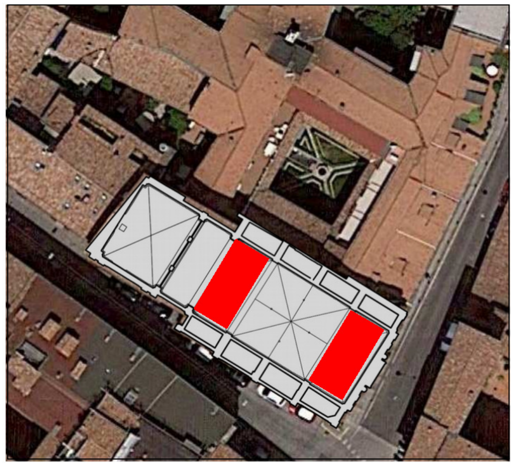

Figure 2. The San Barbaziano church: external view (left) and ground level plan (right).

singular part parallel to the unit vector $\boldsymbol{h}$ normal to Γ, i.e., it is singular transversely to Γ. Hence the directional derivative of the Airy stress function along $\boldsymbol{h}$, namely F_h, has a discontinuity and

$$\boldsymbol{H}_s = \delta(\Gamma) F_h \boldsymbol{h} \otimes \boldsymbol{h}, \qquad \boldsymbol{S}_s = \delta(\Gamma) F_h \boldsymbol{k} \otimes \boldsymbol{k}, \tag{8}$$

where $\boldsymbol{H}_s$ is the singular part of $\boldsymbol{H}$, $\boldsymbol{S}_s$ is that of the Pucher stress, $\boldsymbol{k}$ is the unit vector tangent to Γ, and $\delta(\Gamma)$ is the unit line Dirac delta on Γ. The fold is concave due to the concavity of F_h. A detailed analysis of the model, together with a thorough discussion on the singular stress functions, is presented in [Angelillo et al. 2013].

3. The case study

The case study is the barrel vault with lunette covering the transept of the San Barbaziano, a brick masonry building at the corner of Via Barberia and Via Cesare Battisti in Bologna. It was built between 1608 and 1612 by Pietro Fiorini and designed to include the remains of a late Middle Age monastery church which did not conform to the canons of the Trent council.

The church is formed by a late Mannerist single nave with eight side chapels belonging to the original church, separated by masonry piers and incorporated in the new building at the ground level.

The higher part of the church consists only of the central nave (45 m in length, 11.60 m in width), with external masonry buttresses corresponding to the separation walls of the lower chapels (Figure 2).

The walls are very slender, considering that the façade, apsis walls, and lateral walls of the ground level chapels are 85 cm thick. The longitudinal walls are 40 cm thick at both levels. The three-bay nave is longitudinally counterpointed by two barrel vaults with lunettes and a central bay with a cross vault (Figure 3). A second cross vault covers the apsis [Colla and Pascale 2015]. Attention has been focussed on the thin brick masonry barrel vaults with lunettes (Figure 4).

The membrane behaviour models with good accuracy the thin masonry vaults (thickness 12.5 cm), whose intrados and extrados are approximated by the graphs of the functions derived by the general

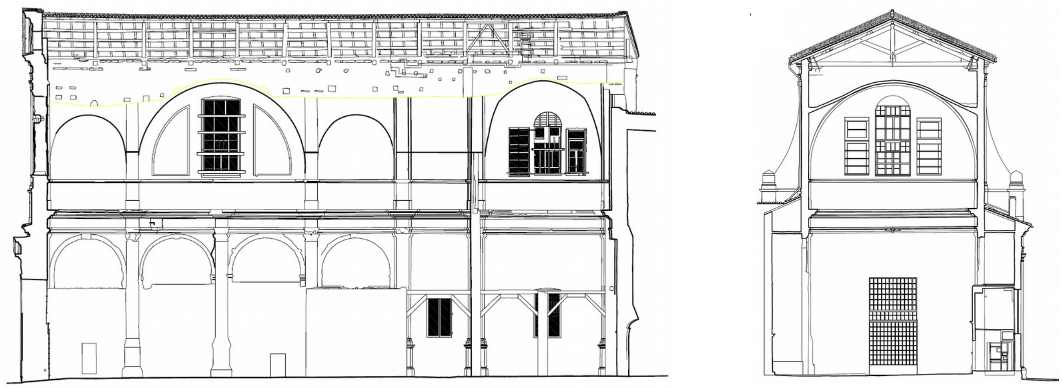

Figure 3. Longitudinal (left) and transversal section (right) of the San Barbaziano church.

Figure 4. Intrados of the barrel vault with lunette in the San Barbaziano church.

surface	coefficients			
main vault intrados		$a = -0.18$	$m = 5.60$	
main vault extrados		$a = -0.14$	$m = 5.73$	
main vault membrane	$a = 1.22 \cdot 10^{-4}$	$d = 3.82 \cdot 10^{-3}$	$g = -0.15$	$m = 5.66$
lunette intrados		$d = -0.35$	$m = 2.80$	
lunette extrados		$d = -0.26$	$m = 2.92$	
lunette membrane	$a = 5.04 \cdot 10^{-4}$	$d = 0.29$	$g = 3.95 \cdot 10^{-3}$	$m = 2.92$

Table 1. Non-null coefficients of the relation (9) for the surfaces' representation.

expression

$$f_i(x_1, x_2) = a_i x_1^2 x_2^2 + b_i x_1^2 x_2 + c_i x_1 x_2^2 + d_i x_1^2 + e_i x_1 x_2 + g_i x_2^2 + h_i x_1 + l_i x_2 + m_i. \tag{9}$$

The choice of the complete biquadratic function has been made in order to implement in the developed numerical procedure a general Monge form of a quadric surface. The numerical coefficients (Table 1) have been chosen in order to represent the surfaces of the main vault and of the lunette membrane, respectively highlighted in brown and cyan in Figure 5 (left), together with the cylindrical extrados and intrados surfaces.

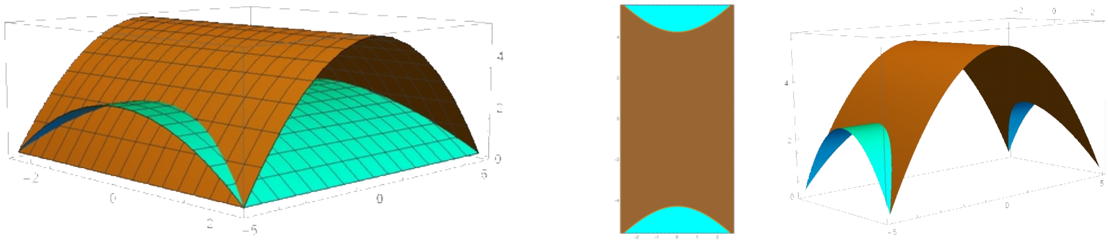

Figure 5. Main vault (brown) and lunette (cyan): surfaces (left), region domains (middle), and combined membrane (right).

The concave stress function $F(x_1, x_2)$ for the uniform vertical pressure $p = 1800\,\mathrm{N}\cdot\mathrm{m}^{-2}$ is given by the solution of the equilibrium equation (5). For the main vault (F^M) and lunette (F^L) vault membrane they are, respectively,

$$\begin{aligned} F^M(x_1,x_2) = &-1.84\cdot 10^6 \log(35.49-x_1)+5.19\cdot 10^4 x_1 \log(35.49-x_1)-1.84\cdot 10^6 \log(35.49+x_1)\\ &-5.19\cdot 10^4 x_1 \log(35.49+x_1)-1.84\cdot 10^6 \log(5.6-x_2)+3.29\cdot 10^5 x_2 \log(5.6-x_2)\\ &-1.84\cdot 10^6 \log(5.6+x_2)-3.29\cdot 10^5 x_2 \log(5.6+x_2), \end{aligned} \tag{10}$$

and

$$\begin{aligned} F^L(x_1,x_2) = &-4.46\cdot 10^5 \log(2.80-x)+1.59\cdot 10^5 x \log(2.80-x)-4.46\cdot 10^5 \log(2.80+x)\\ &-1.59\cdot 10^5 x \log(2.80+x)-4.46\cdot 10^5 \log(24.25-y)+1.84\cdot 10^4 y \log(24.25-y)\\ &-4.46\cdot 10^5 \log(24.25+y)-1.84\cdot 10^4 y \log(24.25+y). \end{aligned} \tag{11}$$

The two Airy stress functions are definite respectively on the two region domains reported in Figure 5 (middle) whose boundaries on the planform are given by the expressions

$$x_2(x_1) = \pm\frac{29.63\sqrt{-9569+1025x_1^2}}{\sqrt{460208+1175x_1^2}}. \tag{12}$$

Considering the rectangular planform, the vertical equilibrium for the combined vaults (9) gives the Pucher stresses obtained by the relation (4). The minimum and maximum Pucher stress maps are reported in Figure 6, while the minimum and maximum physical stresses are reported in Figure 7.

As can be noted, the stress intensity derived from the presented equilibrium solution is very low compared to the possible strength of the masonry, which can be considered ranging between four to six times the calculated values [Faella et al. 2012]. In Figure 7, right, the stress intensity is near the null value, and so the variable distribution is actually due to the numerical approximation of the routine.

A comparison of the obtained equilibrated and admissible stress field with a finite element solution is also reported in order to highlight the effectiveness of the method in describing the vault's behaviour. Analyses based on two-dimensional and three-dimensional finite elements with the linear elastic constitutive model have been performed. The resulting stress maps, with reference to the middle plane of the vault, are reported in Figure 8.

The linear analysis has been considered sufficient to show the reliability of the proposed approach. Note that in order to obtain an equilibrate strain and stress field, the finite element solution needs to

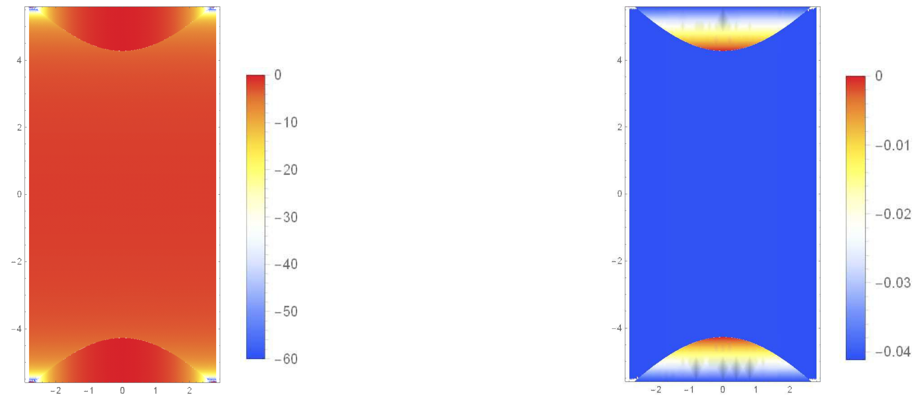

Figure 6. Minimum (left) and maximum (right) Pucher stress maps (values are in $\mathrm{N \cdot cm^{-2}}$).

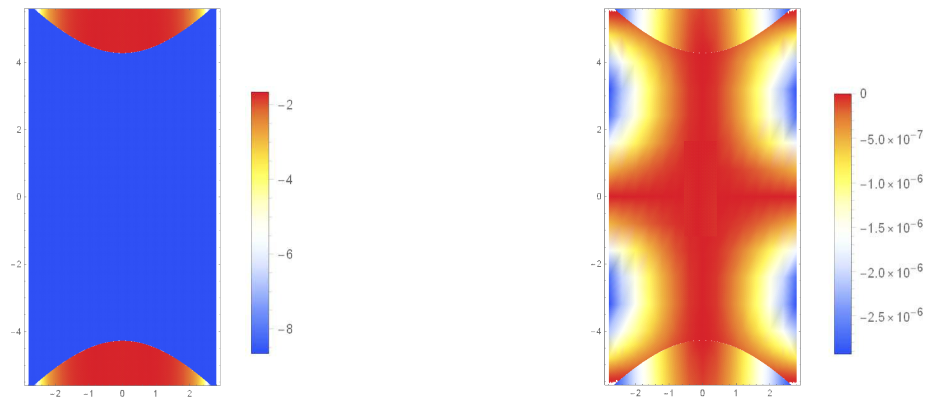

Figure 7. Minimum (left) and maximum (right) physical stress maps (values are in $\mathrm{N \cdot cm^{-2}}$).

account for the bending stiffness of both the main vault and lunette. Despite the general coherence between the finite element and continuous equilibrium solutions, this is an indirect demonstration of the efficiency and robustness of the proposed method, which is based on the safe theorem of limit analysis.

A very low stress level can be detected in the barrels while the maximum stress concentration has been found at the springing of the vaults and at the intersection of the two vaults (Figure 9).

4. Singular stress fields

The main aspect to be considered in the analysis of combined vaults concerns the singular stress fields arising at the intersection Γ of the two vaults (Figure 10, left), i.e., a line Dirac delta with support on the above defined region boundaries (Figure 10, middle).

In particular, the stress tensor has a singular part along the mentioned intersection of the vaults, whose locally normal vector $\boldsymbol{h}$ and tangent vector $\boldsymbol{k}$ are represented in Figure 10 (right), where the domain of the intersection curve on the planfold (dashed red line) is reported together with the intersection curve (continuous line).

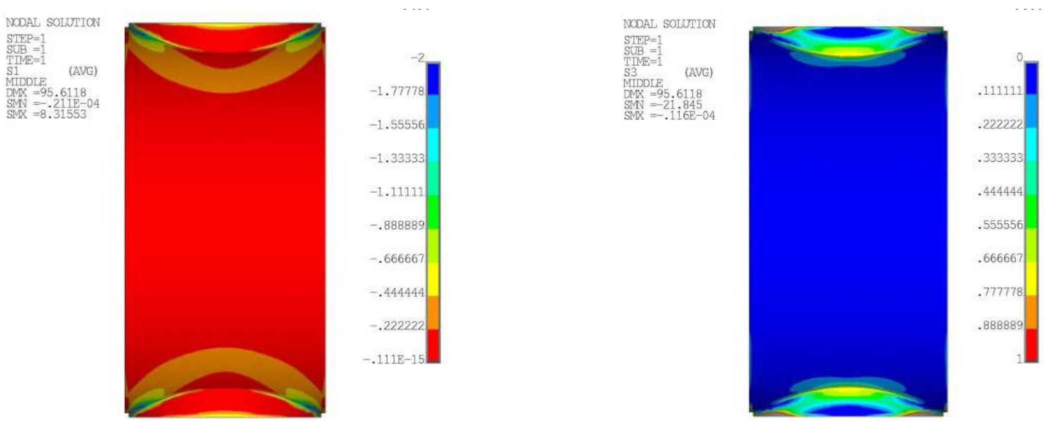

Figure 8. Finite element analysis: minimum (left) and maximum (right) stress maps (values are in $\mathrm{N} \cdot \mathrm{mm}^{-2}$).

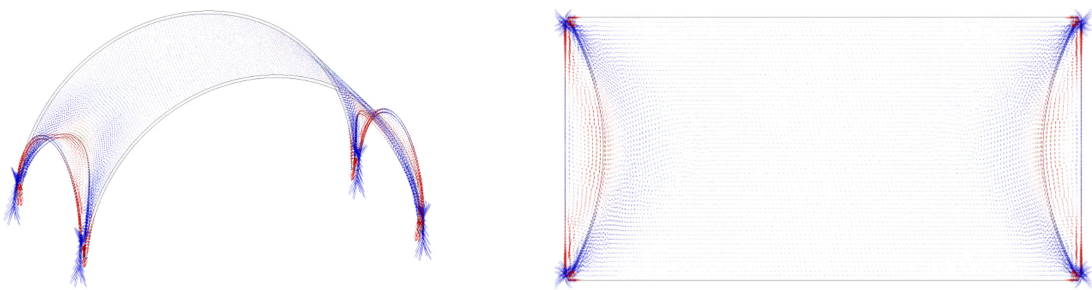

Figure 9. Stress vector maps of the finite element analysis.

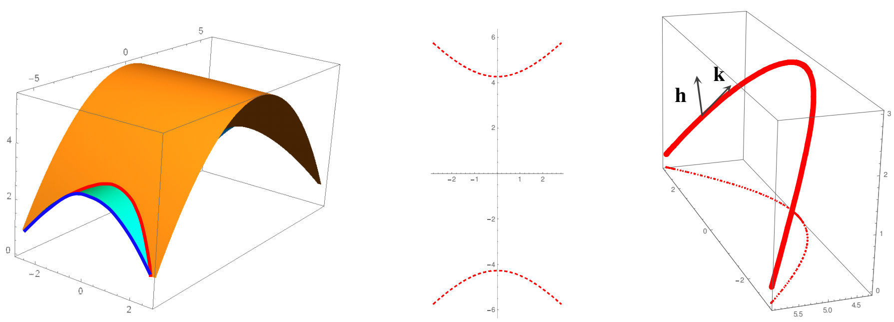

Figure 10. Position of the line Dirac delta at the vaults intersection (left), line plane domain (middle), and plot of the line Γ (right).

As a result, there is an increase in the normal stress along the intersection curve (in red in Figure 10, left and right), compared to the same loading condition in an arch with unitary depth and the same geometry of the lunette, i.e., the directrix curve of the cylindrical vault (in blue in Figure 10).

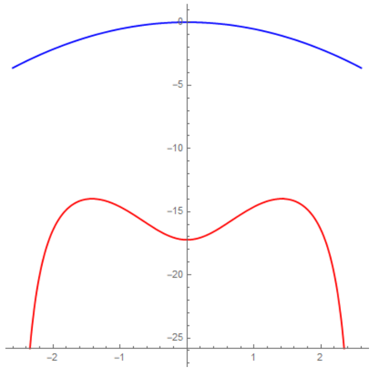

Figure 11. Compressive stress in the intersection curve (red) compared to that in a similar barrel vault (blue).

The compressive stresses in the two cases are shown in Figure 11. Although the ancient builders of combined vaults lacked the appropriate scientific tools to determine this increase, they realized technological details such as the carved stone ribs that counterbalance the stresses maintain the appeal of their constructions.

5. Conclusion

An application of the safe theorem of limit analysis has been presented to model the behaviour of a combined vault system, considered as a continuous material with rigid no-tension constitutive behaviour. The model, based on the definition of a membrane shape function contained in the vault's volume and a stress function formulation, allows the representation of the stress maps relative to an equilibrium solution compatible with the unilateral material assumption. The case study of the barrel vault with lunette in the San Barbaziano church has been examined to show a possible application of the proposed modelling. Special attention has been devoted to the singular stress field arising in the intersection curves for the equilibrium fulfillment. The solutions provided by the proposed method are compared with those obtained by a finite element analysis to assess the efficiency and robustness of the formulation and the ductility of the application in the case of combined vaults, where singular stresses are involved. The proposed procedure allows not only the evaluation of the areas susceptible to damage due to fracture but also the curves where singular stresses are localized, to address the crack pattern of real combined vaulted structures.

Acknowledgements

The contribution of University of Campania "Luigi Vanvitelli" is gratefully acknowledged.

References

[Angelillo 2015] M. Angelillo, "Static analysis of a Guastavino helical stair as a layered masonry shell", *Compos. Struct.* **119** (2015), 298–304.

[Angelillo et al. 2010] M. Angelillo, L. Cardamone, and A. Fortunato, "A numerical model for masonry-like structures", *J. Mech. Mater. Struct.* **5**:4 (2010), 583–615.

[Angelillo et al. 2013] M. Angelillo, E. Babilio, and A. Fortunato, "Singular stress fields for masonry-like vaults", *Contin. Mech. Therm.* **25**:2-4 (2013), 423–441.

[Angelillo et al. 2016] M. Angelillo, E. Babilio, A. Fortunato, M. Lippiello, and A. Montanino, "Analytic solutions for the stress field in static sandpiles", *Mech. Mater.* **95** (2016), 192–203.

[Bartoli et al. 2017] G. Bartoli, M. Betti, P. Biagini, A. Borghini, A. Ciavattone, M. Girardi, G. Lancioni, A. M. Marra, B. Ortolani, and B. Pintucchi, "Epistemic uncertainties in structural modelling: a blind benchmark for seismic assessment of slender masonry towers", *J. Perform. Constr. Fac.* **31**:5 (2017), 04017067.

[Bergamasco et al. 2017] I. Bergamasco, A. Fortunato, A. Gesualdo, A. Iannuzzo, and M. Monaco, "A no-tension model for the analysis of combined masonry vaults", pp. 1387–1395 in *AIMETA 2017 — XXIII Conference of the Italian Association of Theoretical and Applied Mechanics*, vol. 4, 2017.

[Bergamasco et al. 2018] I. Bergamasco, A. Gesualdo, A. Iannuzzo, and M. Monaco, "An integrated approach to the conservation of the roofing structures in the Pompeian *Domus*", *J. Cult. Herit.* **31** (2018), 141–151.

[Block 2009] P. Block, *Thrust network analysis*, PhD thesis, Massachusetts Institute of Technology, 2009.

[Block and Lachauer 2014] P. Block and L. Lachauer, "Three-dimensional (3D) equilibrium analysis of gothic masonry vaults", *Int. J. Archit. Herit.* **8**:3 (2014), 312–335.

[Buonocore et al. 2014] G. Buonocore, A. Gesualdo, M. Monaco, and M. T. Savino, "Improvement of seismic performance of unreinforced masonry buildings using steel frames", in *Proceedings of the Twelfth International Conference on Computational Structures Technology*, vol. 117, edited by B. H. V. Topping and P. Iványi, Civil-Comp Press, Stirlingshire, Scotland, 2014.

[Colla and Pascale 2015] C. Colla and G. Pascale, "Diagnostics and monitoring of the church of San Barbaziano in Bologna", *Key Eng. Mater.* **624** (2015), 147–154.

[Como 1992] M. Como, "Equilibrium and collapse of masonry bodies", *Meccanica* **27**:3 (1992), 185–194.

[Faella et al. 2012] G. Faella, G. Frunzio, M. Guadagnuolo, A. Donadio, and L. Ferri, "The church of the nativity in Bethlehem: non-destructive tests for the structural knowledge", *J. Cult. Herit.* **13**:4 (2012), e27–e41.

[Flügge and Geyling 1957] W. Flügge and F. T. Geyling, "A general theory of deformations of membrane shells", *IABSE publ.* **17** (1957), 23–46.

[Fraternali 2010] F. Fraternali, "A thrust network approach to the equilibrium problem of unreinforced masonry vaults via polyhedral stress functions", *Mech. Res. Commun.* **37**:2 (2010), 198–204.

[Fraternali 2011] F. Fraternali, "A mixed lumped stress-displacement approach to the elastic problem of masonry walls", *Mech. Res. Commun.* **38**:3 (2011), 176–180.

[Fraternali et al. 2014] F. Fraternali, I. Farina, and G. Carpentieri, "A discrete-to-continuum approach to the curvatures of membrane networks and parametric surfaces", *Mech. Res. Commun.* **56** (2014), 18–25.

[Gesualdo and Monaco 2010] A. Gesualdo and M. Monaco, "Seismic vulnerability reduction of existing masonry buildings: modelling of retrofitting techniques", pp. 853–858 in *Urban Habitat Constructions under Catastrophic Events — Proceedings of the COST C26 Action Final Conference*, edited by F. M. Mazzolani, 2010.

[Gesualdo et al. 2010] A. Gesualdo, M. Monaco, and M. T. Savino, "Seismic retrofitting techniques for masonry arch bridges", pp. 859–864 in *Urban Habitat Constructions under Catastrophic Events — Proceedings of the COST C26 Action Final Conference*, edited by F. M. Mazzolani, 2010.

[Gesualdo et al. 2017] A. Gesualdo, C. Cennamo, A. Fortunato, G. Frunzio, M. Monaco, and M. Angelillo, "Equilibrium formulation of masonry helical stairs", *Meccanica* **52**:8 (2017), 1963–1974.

[Hendry 1995] A. W. Hendry, "Masonry arch design at the end of the 19th century", pp. 140–144 in *Proc. 4th Int. Masonry Symp.*, edited by H. W. H. West, Proceedings of the British Masonry Society **7**, 1995.

[Heyman 1966] J. Heyman, "The stone skeleton", *Int. J. Solids Struct.* **2**:2 (1966), 249–256.

[Heyman 1970] J. Heyman, "The collapse of stone vaulting", *WIT Trans. Built Environ.* **4** (1970), 12 pp.

[Heyman 1977] J. Heyman, *Equilibrium of shell structures*, Clarendon Press, Oxford, 1977.

[Heyman 1982] J. Heyman, *The masonry arch*, Ellis Horwood Limited, Chichester, England, 1982.

[Hooke 1676] R. Hooke, *A description of helioscopes, and some other instruments*, 1676.

[Huerta 2001] F. S. Huerta, “Mechanics of masonry vaults: the equilibrium approach”, pp. 47–69 in *Proceedings of 3rd International Seminar on Historical Constructions* (Guimarães, 2001), edited by P. B. Lourenço and P. Roca, 2001.

[Huerta 2008] S. Huerta, “The analysis of masonry architecture: a historical approach”, *Architect. Sci. Rev.* **51**:4 (2008), 297–328.

[Iannuzzo et al. 2018] A. Iannuzzo, M. Angelillo, E. De Chiara, F. De Guglielmo, F. De Serio, F. Ribera, and A. Gesualdo, “Modelling the cracks produced by settlements in masonry structures”, *Meccanica* **53**:7 (2018), 1857–1873.

[Kurrer 2008] K.-E. Kurrer, *The history of the theory of structures: from arch analysis to computational mechanics*, Ernst & Sohn, Berlin, 2008.

[Lucchesi et al. 2007] M. Lucchesi, C. Padovani, G. Pasquinelli, and N. Zani, “Static analysis of masonry vaults, constitutive model and numerical analysis”, *J. Mech. Mater. Struct.* **2**:2 (2007), 221–244.

[Lucchesi et al. 2008] M. Lucchesi, M. Šilhavý, and N. Zani, “Integration of measures and admissible stress fields for masonry bodies”, *J. Mech. Mater. Struct.* **3**:4 (2008), 675–696.

[Lucchesi et al. 2012] M. Lucchesi, M. Šilhavý, and N. Zani, “On the choice of functions spaces in the limit analysis for masonry bodies”, *J. Mech. Mater. Struct.* **7**:8-9 (2012), 795–836.

[Marmo and Rosati 2017] F. Marmo and L. Rosati, “Reformulation and extension of the thrust network analysis”, *Comput. Struct.* **182** (2017), 104–118.

[Marmo et al. 2018] F. Marmo, D. Masi, and L. Rosati, “Thrust network analysis of masonry helical staircases”, *Int. J. Archit. Herit.* **12**:5 (2018), 828–848.

[Moseley 1833] H. Moseley, “On the equilibrium of the arch”, *Cambridge Philos. Trans.* **5** (1833), 293–313.

[Moseley 1860] H. Moseley, *The mechanical principles of engineering and architecture*, Wiley, New York, 1860.

[O’Dwyer 1999] D. O’Dwyer, “Funicular analysis of masonry vaults”, *Comput. Struct.* **73**:1-5 (1999), 187–197.

[Pucher 1934] A. Pucher, “Über der Spannungszustand in gekrümmten Flächen”, *Beton u. Eisen* **33** (1934), 298–304.

[Pucher 1937] A. Pucher, “Die Berechnung von doppelt gekrümmten Schalen mittels Differenzengleichungen”, *Der Bauingenieur* **18**:9-10 (1937), 118–123.

[Sacco et al. 2018] E. Sacco, D. Addessi, and K. Sab, “New trends in mechanics of masonry”, *Meccanica* **53**:7 (2018), 1565–1569.

Received 12 Nov 2018. Revised 24 Jan 2019. Accepted 2 Mar 2019.

MICHELA MONACO: michela.monaco@unicampania.it
Department of Architecture and Industrial Design (DADI), University of Campania “Luigi Vanvitelli”, Aversa, Italy

IMMACOLATA BERGAMASCO: immacolata.bergamasco@beniculturali.it
Archaeological Park of Pompeii, Ministry for Cultural Heritage and Activities and Tourism, Pompeii, Italy

MICHELE BETTI: michele.betti@unifi.it
Department of Civil and Environmental Engineering, University of Florence, Florence, Italy

JOURNAL OF MECHANICS OF MATERIALS AND STRUCTURES

msp.org/jomms

Founded by Charles R. Steele and Marie-Louise Steele

Cover photo: Wikimedia Commons

See msp.org/jomms for submission guidelines.

JoMMS (ISSN 1559-3959) at Mathematical Sciences Publishers, 798 Evans Hall #6840, c/o University of California, Berkeley, CA 94720-3840, is published in 10 issues a year. The subscription price for 2018 is US $615/year for the electronic version, and $775/year (+$60, if shipping outside the US) for print and electronic. Subscriptions, requests for back issues, and changes of address should be sent to MSP.

JoMMS peer-review and production is managed by EditFlow® from Mathematical Sciences Publishers.

PUBLISHED BY

mathematical sciences publishers

nonprofit scientific publishing

http://msp.org/

Journal of Mechanics of Materials and Structures

Volume 13, No. 5 December 2018

Special issue on
Structural Analysis of Real Historic Buildings (part 1)

1559-3959(2018)13:5;1-X